International Journal of Plasticity 26 (2010) 84–92

Contents lists available at ScienceDirect

International Journal of Plasticity

journal homepage: www.elsevier.com/locate/ijplas

Low temperature deformation in iron studied with dislocation dynamics simulations

S. Naamane [a], G. Monnet [a,*], B. Devincre [b]

[a] EDF-R&D, MMC, Avenue des Renardières, 77818 Moret sur Loing, France
[b] LEM, CNRS-ONERA, 29 av. de la Division Leclerc, 92130 Châtillon, France

ARTICLE INFO

Article history:
Received 12 December 2008
Received in final revised form 7 May 2009
Available online 18 May 2009

Keywords:
Dislocations
Dislocation dynamics simulations
Iron
Low temperature
Thermal activation

ABSTRACT

Tensile tests of iron single crystals reported in the literature were analyzed to deduce the effective stress associated to the double-kinks mechanism in order to establish a mobility law for screw dislocations. This mobility law is used to carry out the first dislocation dynamics simulations of low temperature deformation in iron. The sensitivity of the flow stress on temperature and strain rate is investigated and compared to experiment. First simulation results give an insight into the effect of temperature on the microstructure evolution and on the dislocation–dislocation interactions.

1. Introduction

In iron at low temperature, the flow stress is strongly temperature dependent (Kossowsky and Brown, 1966; Kubin, 1976; Smidt, 1969; Spitzig and Keh, 1970a; Stein et al., 1963). The microstructure of strained specimens is essentially formed of long and straight screw segments (Solomon and McMahon, 1966). This anisotropy of the dislocation microstructure directly reflects the anisotropy of the dislocation mobility. The screw dislocations move slower than dislocations of other characters. The mobility of screw dislocations is therefore expected to control the plastic flow in iron. The motion of screw dislocations occurs through the nucleation and the propagation of double kinks (DK) along their lines. The double-kinks mechanism is a thermally activated process, which explains the strong temperature dependency of the flow stress in iron.

Several investigations were dedicated to the modelling of the DK mechanism (Domain and Monnet, 2005; Louchet and Kubin, 1979; Wen and Ngan, 2000; Yang and Moriarty, 2001). The main objective was to deduce the activation energy of the formation of the DK as a function of the effective stress. In order to compare with experiment, the effective stress was estimated from the Critical Resolved Shear Stress (CRSS) considered equal to the yield stress obtained from the stress–strain curves of tensile-deformed iron single crystals. However, as pointed out first by Solomon and McMahon (1966) and Brown and Ekvall (1962), the CRSS corresponding to the movement of screw dislocations may differ from the conventional yield stress. We expect this point to be at the origin of the disparity in experimental results found in the literature.

The objective of the present work is to establish and validate thermally activated dislocations mobility laws that can be used in mass dislocation dynamics (DD) simulations. The ultimate goal of the present work is to undertake investigations on the mechanical properties of iron at low temperature. A new method for the determination of the CRSS and the associated activation energy are given, respectively, in Sections 2 and 3. In the subsequent section, we show how the mobility law of

* Corresponding author. Tel.: +33 (0) 1 60 73 64 73; fax: +33 (0) 1 60 73 68 89.
E-mail addresses: ghiath.monnet@edf.fr, ghiathmonnet@yahoo.fr (G. Monnet).

0749-6419/$ - see front matter © 2009 Published by Elsevier Ltd.
doi:10.1016/j.ijplas.2009.05.003

screw dislocations is deduced following a method already applied in the case of tantalum (Tang et al., 1998) and zirconium (Monnet et al., 2004). DD results are analyzed and compared with experiment in Section 5. In the last section, we show as a first application, the effect of temperature on dislocation–dislocation interactions.

2. Determination of the CRSS

Solomon and McMahon (1966) and Brown and Ekvall (1962) drew attention to the large extent of stage 0 in iron at low temperature. Their results demonstrate that the deviation from the elastic loading of single crystals corresponds to the threshold of movement of non-screw dislocations. Stage 0 extent is a function of the initial density of non-screw dislocations. The deformation accommodated in this stage is anelastic, i.e., of a dissipative nature but reversible from a mechanical point of view. The threshold of this stage, called "microyield stress", was unfortunately confused with the yield point estimated according to the conventional method (i.e., $R_{0.2\%}$). Therefore, the values of the CRSS provided in the literature do not correspond to the real yield point associated to the irreversible character of plastic deformation. Furthermore, the exhaustion of the mobile non-screw dislocations is assumed to be responsible for the large stress increase rate observed in stage 0. Consequently, this increase cannot be interpreted as a strain hardening, since it does not involve the dislocation–dislocation interactions controlling the latter stages of plastic strain. The flow stress to be identified as the CRSS, should then be taken at the end of stage 0.

In order to do this, we gathered all available experimental stress–strain curves of iron single crystals tested at a wide temperature range. Only samples with orientations close to the center of the standard triangle are selected in this treatment in order to ensure that only the $\{1\,1\,0\}\langle 1\,1\,1\rangle$ slip systems are activated. All these orientations had a Schmid factor about 0.5 and the tensile tests were almost performed at a strain rate close to $10^{-4}\,s^{-1}$.

In Fig. 1, we show the evolution of the CRSS, defined at the end of Stage 0, and the microyield stress values obtained for iron single crystals with different carbon content: <2 at. ppm (Quesnel et al., 1975; Spitzig, 1973), 6 at. ppm (Kuramoto et al., 1979), 10 at. ppm (Spitzig and Keh, 1970b) and 37 at. ppm which also contains about 0.16 wt.% of Ti (Spitzig and Keh, 1970b).

In this figure, we can see that the values of the CRSS are substantially larger than the values of the microyield stress. The CRSS becomes constant beyond a given temperature, named T_a in the following. This temperature belongs to the interval 300–400 K. In addition, in the investigated carbon content range, the CRSS is found to be less sensitive to carbon content than the microyield stress.

3. Experimental determination of the activation energy

The DK mechanism consists of the nucleation and the propagation of a pair of kinks along a dislocation line. At low temperature, this process is controlled by the nucleation step (Seeger and Schiller, 1962). The rate is assumed to follow an Arrhenius-type equation in which the activation energy corresponds to the free Gibbs energy required to displace a segment of dislocation to the next Peierls valley. This energy can be considered equal to the activation enthalpy only when the activation entropy is negligible (Schoeck, 1965). The main contribution to the latter is related to the temperature dependency of the shear modulus (Schoeck, 1965; Conrad and Wiedersich, 1960). In the case of iron, Spitzig and Keh, 1970a,b found that the free enthalpy is proportional to the temperature and that the activation entropy is within 5% of the total activation energy. It follows that, for iron, the Gibbs free energy associated with the DK nucleation can be approximated by the corresponding activation enthalpy.

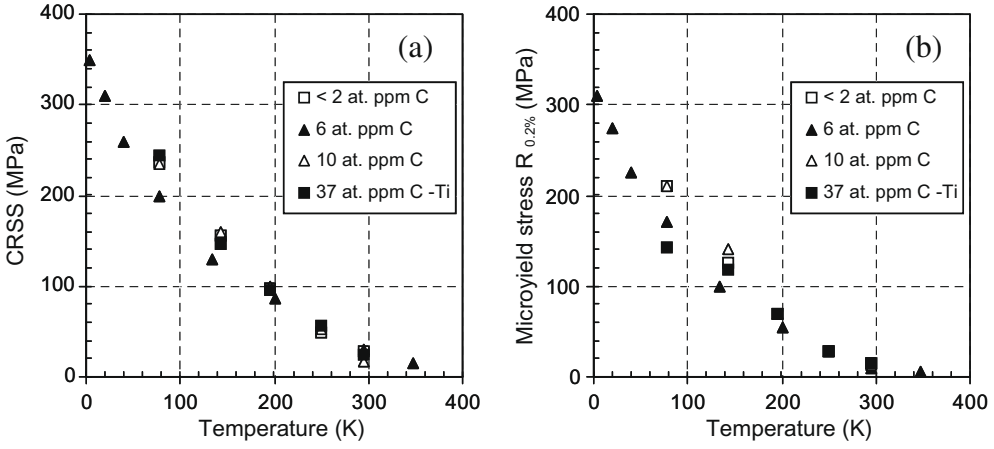

Fig. 1. Effect of temperature on the CRSS (a) and the microyield stress ($R_{0.2\%}$) (b) in iron with different carbon content (experimental values).

The activation enthalpy can be obtained from mechanical tests (Spitzig and Keh, 1970a,b; Tang et al., 1998). It was experimentally found to be proportional to the temperature (Spitzig, 1973; Schoeck and Nabarro, 1980), $\Delta H = CkT$, where C is a constant and k the Boltzmann's constant. It decreases strongly with the effective stress, τ^*. We should note here that the effective stress is deduced from the CRSS by subtracting the internal stress τ_μ, which is a component independent of the lattice friction, i.e., forest or precipitates obstacles, that can be overcome owing to the dislocation curvature. The corresponding stress, τ_μ, is then athermal and should be proportional to the shear modulus, which varies slightly with temperature (Ghosh and Olson, 2002). In the following, a simple formula is used to compute the shear modulus as a function of temperature: $\mu = 87.6–0.017\ T$ (in GPa and T in absolute temperature). From experimental results (Spitzig and Keh, 1970b), we could estimate τ_μ to be close to 8 MPa at 300 K.

Use is made of the phenomenological formula of Kocks et al. (1975) to express the dependency of the activation enthalpy on the effective stress:

$$\Delta H = \Delta H_0 \left(1 - \left(\frac{\tau^*}{\tau_o}\right)^p\right)^q \tag{1}$$

where τ_o is a parameter corresponding to the extrapolation of τ^* at the absolute zero temperature, ΔH_0 is the total activation enthalpy necessary to overcome the lattice resistance without the help of external forces. p and q are two fitting parameters. This expression was previously used in the case of tantalum (Tang et al., 1998) and zirconium (Monnet et al., 2004), which experience a similar thermally activated motion of screw dislocations. The results of the fitting procedure yields $\Delta H_0 = 0.84$ eV, $\tau_o = 363$ MPa, $p \approx 0.5$ and $q \approx 1$. The activation enthalpy can then be simply written as follows:

$$\Delta H = \Delta H_0 \left(1 - \sqrt{\frac{\tau^*}{\tau_o}}\right) \tag{2}$$

This fitting result is drawn in Fig. 2, where Eq. (2) is compared to experimental values of the activation enthalpy. We see that Eq. (2) describes well the whole range of the effective stress. The value of the total activation energy, ΔH_0, is in agreement with other estimations (Spitzig and Keh, 1970a,b). However, in this paper the authors consider the value of τ_o as a simple fitting parameter. It should not be regarded as the effective stress at zero absolute temperature. At very low temperature, say of the order of few absolute degrees, it is less probable that the DK mechanism is activated in real deformation conditions. On the one hand, in most cases, the observed deformation mechanism is twining and, on the other hand, MD simulations (Chaussidon et al., 2006) using different empirical potentials (Ackland et al., 1997; Mendelev et al., 2003) indicate that the critical stress at zero temperature is much larger than all measured values in experiment. A value $\tau_o = 363$ MPa, although in the good experimental range, is not commented further.

Eq. (2) is in good agreement with the experimental measurements made by Smidt (1969), where ΔH is found proportional to the temperature and the ratio $\Delta\tau/\Delta T$ varies linearly with temperature. Hereafter, we note that the square root dependency of the activation energy on the effective stress has a solid theoretical foundation. The critical assumption considered in these theoretical approaches is the shape of the dislocation line during the collective jump of atoms. All predictions of critical shapes of the dislocation line involve the Peierls potential which is, precisely the unknown of the problem, see for example, Dorn and Rajnak (1964). Especially, this potential depends strongly on the inclination of the kink, i.e., on the dislocation shape. A method was proposed to overcome this difficulty by assuming the formation energy of the kink-pair to be independent of stress. This is the corner idea of the models developed, separately, by Hirth and Lothe (1982) and by Schoeck and

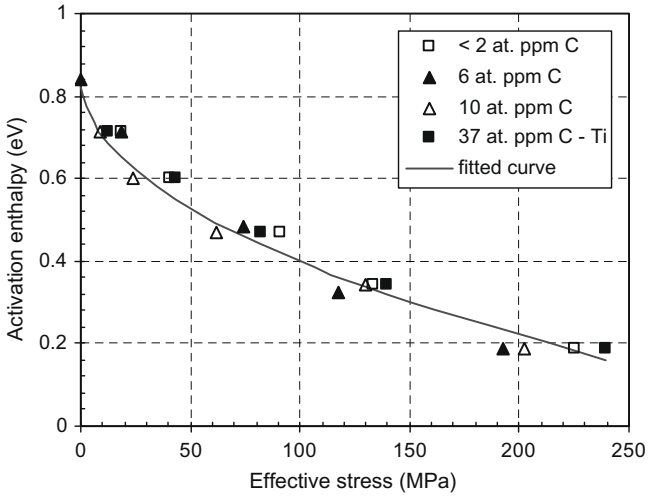

Fig. 2. Evolution of the activation enthalpy as function of the effective stress for iron with different carbon content. The solid lines represent Eq. (2).

Nabarro (1980). Two implicit conditions are behind this assumption: the spacing between the two kinks should be at least larger than twice the width of the kink and the dislocation jump should not exceed one Peierls valley. This regime is expected to prevail at low stresses. In such a configuration, the activation energy is obtained by subtracting the work of the applied stress from the total formation energy of a DK. The latter is considered to be the sum of twice the kink energy and the interaction energy between the two kinks of opposite sign. The model predicts the activation energy associated to the critical separation of the two kinks. The resulting expression involves the square root of the effective stress, in agreement with Eq. (2). It is thus, a priori, surprising to see that Eq. (2) is still valid at large stresses.

In a recent investigation, Domain and Monnet (2005) have studied the screw dislocation motion in iron using molecular dynamics (MD) simulations. They show that the stable configuration of DK for both high stresses and low temperature (down to 12 K) is always characterized by a well-separated kink pair. In addition, they could observe only jumps of one Peierls valley at each thermally activated process. Eq. (2) and so far the models (Schoeck and Nabarro, 1980; Hirth and Lothe, 1982) are thus expected to apply even at low temperature, down to 12 K.

4. Dislocation mobility law at the mesoscopic scale

At the mesoscopic scale, the atomic character of the DK mechanism can hardly be accounted for, since we are interested in the properties of a large number of dislocations at much larger time scale than that characteristic of atomic vibration. The two scales can be bridged (Domain and Monnet, 2005) using an Arrhenius-type rate equation, giving the average dislocation mobility as a function of stress and temperature (Tang et al., 1998; Monnet et al., 2004). More exactly, backward jump frequency being no longer negligible at low stresses, a more appropriate hyperbolic sine function should be employed, see for example (Nabarro, 2003; Zbib et al., 2000). Using the fitted activation energy found in Section 3, the velocity law of screw dislocations can be written as following:

$$v(\tau^*, T) = HL \exp\left(-\frac{\Delta H_0}{kT}\right) \sinh\left(\frac{\Delta H_0}{kT}\sqrt{\frac{\tau^*}{\tau_0}}\right) \tag{3}$$

where, v is the velocity of a screw dislocation segment of length L, H is a constant frequency that can be calculated as explained by Tang et al. (1998) and equals $1.5 \times 10^{11}\ s^{-1}$ in iron. We can note here that Eq. (3) delivers a zero velocity for a zero effective stress, which is not the case for an Arrhenius-type rate equation (Tang et al., 1998; Monnet et al., 2004). This expression is expected to well represent the mobility of screw dislocations in the low temperature regime (up to 300 K).

It should be complemented with a second mobility law for non-screw dislocations. However, the latter can hardly be measured owing to the large velocity of non-screw dislocations and to the fact that their motion is not known to control any mechanical propriety at low temperature. Moreover, the mobility of edge dislocations is expected to depend on the carbon content. Hence, non-screw dislocation mobility is difficult to express and one can only assume that their velocity is much higher than that of screw dislocations. On the other hand, it is worth noticing that Monnet et al. (2004) tested several types of stress vs. velocity laws for non-screw dislocations in zirconium that exhibits mainly the same behavior as iron at low temperature. They found that the simulated flow stress is not affected as long as the mobility of non-screw dislocations is considerably larger than the mobility of screw dislocations. Therefore, for the sake of simplicity, we assume that the velocity of non-screw dislocations is proportional to that of a screw dislocation segment of 1 μm length, with a factor of proportionality (Monnet et al., 2004), $K \gg 1$. The only condition to be fulfilled is that the value of the factor K should decrease with temperature since the difference between the mobility of screw and non-screw dislocations decreases. At the beginning of the athermal plateau, i.e., when $T = T_a$, the difference should vanishes ($K = 1$) in order to confer to dislocations of all characters the same mobility. The main difficulty with this solution is the setting of a reference K value at the lowest simulated temperature. In the case of zirconium, several values of K, were tested and simulation results were found independent of this parameter (Monnet et al., 2004). In this work, we also performed simulations with different values of K and the flow stress was found poorly affected.

The initial configuration of the simulations contains a random distribution of dipolar dislocation loops, i.e., formed of only edge dislocations belonging to the 12 $\{1\,1\,0\}\langle 1\,1\,1\rangle$ slip systems. The idea behind such initial microstructure is to avoid artificial stress singularity at the ending points of Frank–Read sources and to make the initial dislocation microstructure as close as possible to a Frank 3D network. The initial densities of the primary system and forest systems are, respectively, $2.3 \times 10^{10}\ m^{-2}$ and $1.3 \times 10^{11}\ m^{-2}$. Imposing a small dislocation density on the primary slip system allows us (i) to generate a microstructure at the yield point close to that observed experimentally, i.e., made basically of screw dislocations and (ii) to reach at the CRSS a dislocation density on the primary slip system about $10^{12}\ m^{-2}$, which is the density of reference used to fit Eq. (3) on experimental data. To avoid strong self-dislocation interactions caused by the application of periodic boundary conditions, we adopt the procedure used by Queyreau et al. (2009) allowing to rotate the crystal axes from the orthogonal axes of the simulation box. This simulation box is of an orthorhombic shape ($10 \times 6 \times 6\ \mu m^3$) that ensures, thanks to periodic boundary conditions, a mean free-path before dislocation self-annihilation of a few tens of micrometers (33 μm) (Monnet et al., 2004). Loading conditions were selected in order to simulate a tensile test at a fixed strain rate, $10^{-4}\ s^{-1}$. In Fig. 3, we show the loading curves for two simulations performed at 50 K for two different K values, 1000 and 10,000. As it can be seen, the simulated flow stress is only weakly affected when changing the value of K with a factor of ten. Additional important parameters used in the DD simulations are the Poisson's ratio $\nu = 0.33$ and the Burgers vector $b = 0.248$ nm.

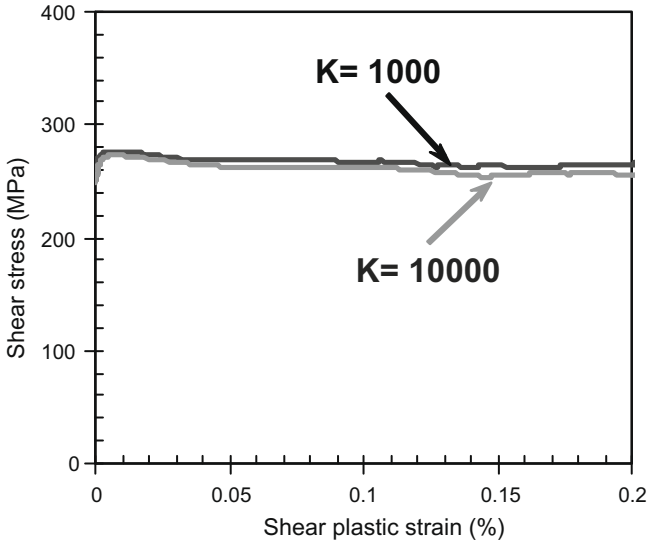

Fig. 3. The simulated stress–strain curves with two different values of K. Simulations were performed at 50 K and considering a fixed strain rate ($10^{-4}\,s^{-1}$).

In the following, we present some applications of the DD simulations compared with experiment that can be considered as a validation of our mobility law. The details of the technique used in the DD simulations can be found elsewhere (Devincre, 1996; Devincre et al., 2001). We just need to recall that in these simulations, the treatment of junctions and other dislocation–dislocation interactions is based on the principle of superposition of the elastic theory. In the case of iron, no modification in these rules is required when compared to those employed for FCC crystals, since junction zipping and unzipping is basically controlled by the variation of elastic energy (Devincre et al., 2001; Queyreau et al., 2009).

5. DD simulations: effect of temperature on the critical stress

Fitting Eq. (3) on experimental data, is based on implicit assumptions: (i) the athermal component of the CRSS is only proportional to the shear modulus, i.e., interaction with carbon atoms and forest interactions are poorly temperature dependent; (ii) the edge dislocation mobility does not affect the CRSS and (iii) the mobility of screw dislocation is controlled by the nucleation process rather than the propagation of kink-pairs. A validation of these assumptions can be performed using DD simulations. If massive DD simulations using Eq. (3) and accounting for all these elementary features can reproduce the experimentally observed evolution of the CRSS as a function of temperature, one proves that only the nucleation process of kink-pairs on screw dislocations controls the CRSS. In order to do so, we design a given initial microstructure, close to the known experimental microstructure and, then, we perform mass DD simulations of tensile mechanical tests in the conditions identical to experiment.

The initial microstructure is identical to the one used for the tests reported in the previous section. The tensile axis is chosen in the center of the standard triangle of the stereographic projection; hence single slip is imposed and the Schmid factor of the primary slip system is 0.5. All the simulations are performed at a fixed strain rate, $10^{-4}\,s^{-1}$. The factor K was selected using the following analysis. At the temperature of 300 K, K is taken equal to unity and at $T = 50$ K, it is taken equal to 1000. Then, a simple linear interpolation is considered to deduce the value of K at intermediate temperatures. Such solution was chosen for reason of simplicity but it is not based on a physical basis since no information about the mobility of non-screw dislocations is at our disposal. In Fig. 4, we show the simulated stress–strain curves at different temperatures. These curves show a small multiplication yield point as a result of the relatively low density of mobile dislocations we introduced in the initial simulation configuration. At larger strains, the flow stress is constant since the dislocation density in the non-active slip systems remains constant. The value of this constant flow stress is defined as the CRSS of our simulations.

In Fig. 5, we plot the computed CRSS in comparison with experimental values. We see that DD simulations reproduce well the sensitivity of the CRSS to temperature in the temperature range [50, 250 K].

Beyond this interval of temperature we believe that the mobility of screw dislocations is controlled not only by the nucleation of DK, but also by the drift velocity of these kinks. The nucleation frequency is too large and the screw dislocation line acquires some curvature under the effect of the applied stress (Tang et al., 1998). The mobility law should therefore account for two rate-controlling processes: the nucleation and propagation of DK. This results in a viscous mobility, leading to a proportionality between the velocity and the stress. Since we are interested in the low temperature regime, we did not implement such mobility law in our simulation. Fig. 5 is considered as a good validation of our DD simulations and mobility laws. In parallel, we investigate the effect of the strain rate on the flow stress. Simulation conditions are the same as mentioned

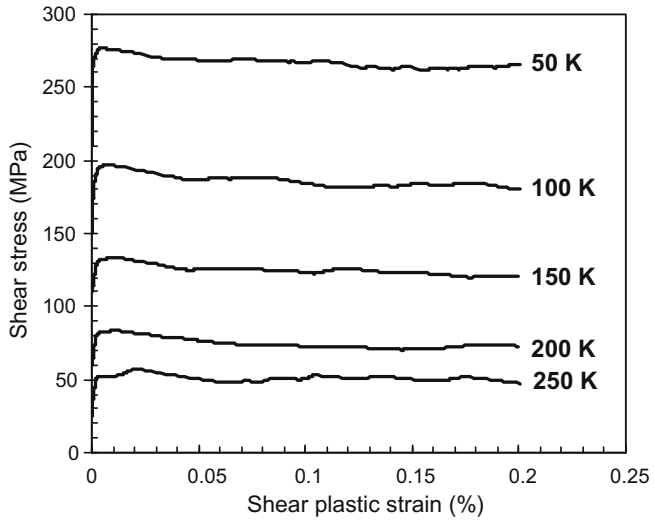

Fig. 4. The simulated stress–strain curves performed in the temperature range 50–250 K. The strain rate considered is $10^{-4}\,s^{-1}$.

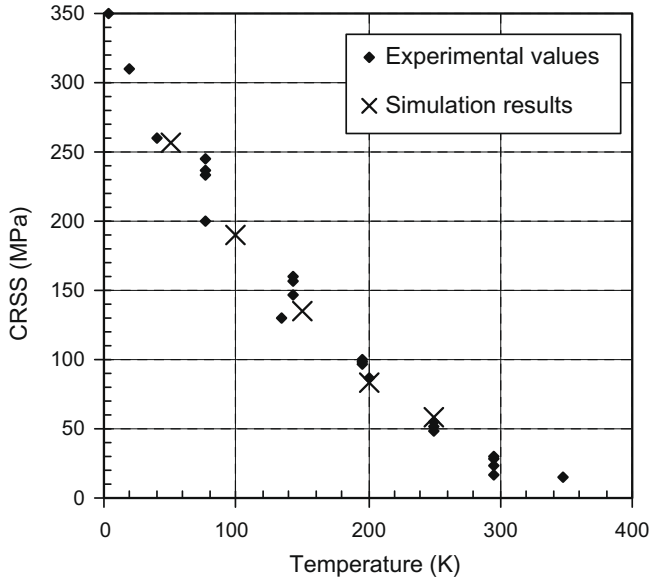

Fig. 5. Temperature dependence of the CRSS under a constant imposed strain rate of $10^{-4}\,s^{-1}$. The DD simulation results are compared to the experimental data obtained for iron with different carbon content.

before, but pre-deformation is first applied to increase the dislocation density. During these tests, the strain rate was increased from 10^{-4} to $10^{-3}\,s^{-1}$. In Fig. 6, we show the stress–strain curves of two simulations performed at 100 K. The evolution of the microstructure is found similar in both cases. This is why we can estimate the activation volume from these two curves.

Measuring the response in stress to this change in strain rate and using the expression of the activation volume:

$$V = kT\Delta \ln(\dot{\gamma})/\Delta\tau|_{T=100\ \mathrm{K}} \tag{4}$$

one finds $V = 17\ b^3$. This value is in good agreement with the input value deduced from Eq. (2) where $V = -\partial H/\partial T|_{T=100K} = 17b^3$. Spitzig and Keh (1970a) found about the same value from experiments on single crystals and Quesnel et al. (1975) deduced a near value of $22\ b^3$.

Finally, Figs. 5 and 6, indicate that our DD simulations well reproduce the sensitivity of the flow stress to temperature and strain rate. This result shows that the thermally activated properties adopted in our simulations capture properly the main features of dislocations behavior at low temperature in iron.

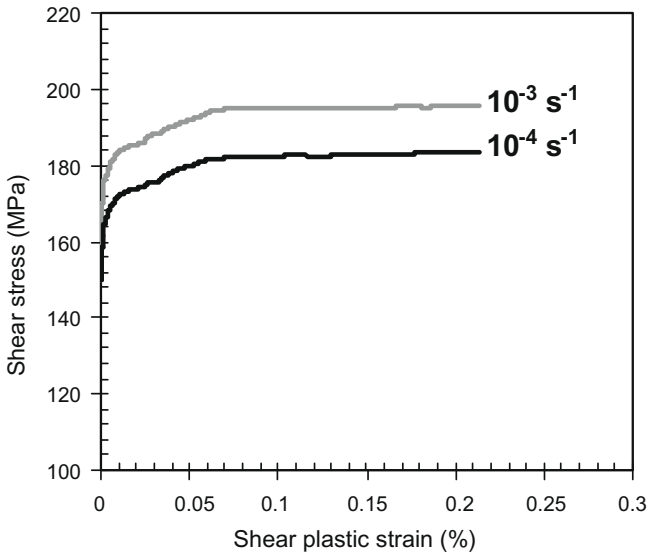

Fig. 6. Simulated stress–strain curves at $T = 100$ K with two different imposed strain rates (10^{-4} and 10^{-4} s^{-1}). Reader must notice that no multiplication yield is reproduced during these two tests since the dislocation microstructure used as initial configuration was predeformed.

6. DD simulations: effect of temperature on dislocation interactions

In this section, we use the same simulation conditions as before. Here, we focus on the simulated microstructure obtained in two different calculations performed at 50 and 250 K. In Fig. 7, the respective dislocation microstructures are shown in a

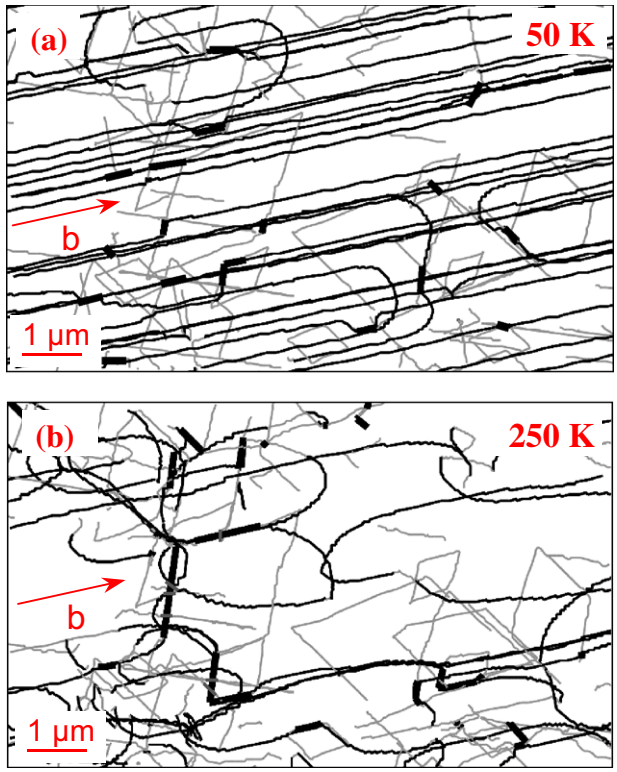

Fig. 7. Simulated dislocation microstructure after a tensile test with a constant imposed strain rate of 10^{-4} s^{-1} at 50 K for (a) and 250 K for (b). The foil of thickness 1 μm cut from the simulation cell along the (1 1 0) slip plane. The bold lines represent junctions formed between the primary (black lines) and forest dislocations (gray lines).

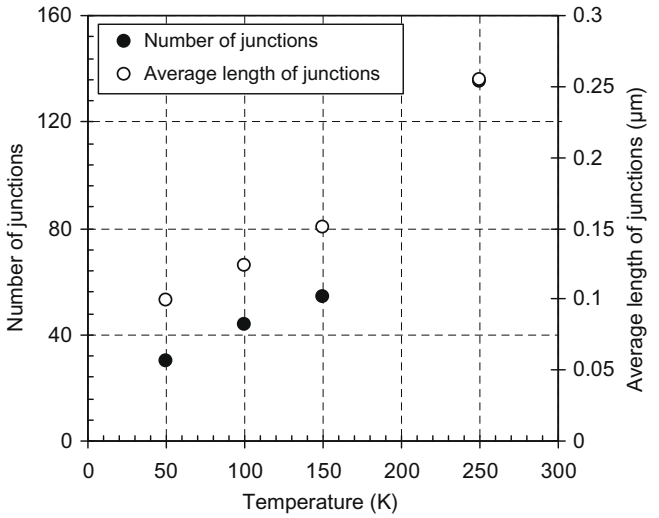

Fig. 8. Number and average length of stable junctions formed in the performed simulations as function of temperature. All calculations are taken from microstructures formed at 0.07% of plastic shear strain.

thin foil of 1 μm thickness parallel to the primary slip system. This figure shows that, at the same plastic strain level, temperature strongly affects the microstructure.

On the one hand, screw dislocations exhibit marked curvature at 250 K and the density of non-screw dislocations is large compared to the lower temperature deformation. On the other hand both the number of junctions and the average junction length are found to increase with temperature. This evolution is illustrated in Fig. 8 that presents the variation of the number and the average length of junctions as function of temperature at the same plastic strain.

These results suggest that the strength of forest interactions decreases significantly when temperature decreases. Of course, the flow stress increases at low temperature, but lattice friction is only responsible for this behavior.

To summarise: when the temperature decreases, the difference between the mobility of screw and non-screw dislocations increases, which leads on the microstructure level to two tendencies: (i) the microstructure becomes formed of long and straight screw dislocations and (ii) the junctions are less numerous and less extended.

However, the associated mechanisms are complex and inter-correlated. In order to quantify the temperature effect, the forest strength should be expressed not only as a function of the interaction nature, but also as a function of temperature and strain rate. This task is under investigation and will be the subject of a forthcoming paper.

7. Conclusions

This paper presents the first dislocation dynamics simulations of low temperature deformation in iron. The crucial task behind this work is the construction of mobility laws for screw and non-screw dislocations. A new analysis of the experimental stress–strain curves of tensile-deformed iron single crystals confirms that the activation energy of the double-kinks mechanism is a square root function of the effective stress, in agreement with most of theoretical models. Using these mobility laws, DD simulations were found to correctly reproduce the dependency of the flow stress on temperature and strain rate.

Primary mass DD simulations suggest that, while the effective stress increases strongly with decreasing temperature, the athermal stress component decreases slowly owing to the difficulty to zip junctions.

References

Ackland, G.J., Bacon, D.J., Calder, A.F., Harry, T., 1997. Computer simulation of point defect properties in dilute Fe–Cu alloy using a many-body interatomic potential. Philos. Mag. A 75, 713–732.
Brown, N., Ekvall, R.A., 1962. Temperature dependence of the yield points in iron. Acta Metall. 10, 1101–1107.
Chaussidon, J., Fivel, M., Rodney, D., 2006. The glide of screw dislocations in bcc Fe: molecular statics and dynamics simulations. Acta Mater. 54, 3407–3416.
Conrad, H., Wiedersich, H., 1960. Activation energy for deformation of metals at low temperatures. Acta Metall. 8, 128–130.
Devincre, B., 1996. Computer simulation in materials science. In: Kirchner, H.O., Pontikis, V., Kubin, L.P. (Eds.), Computer Simulation in Materials Science. NATO ASI Series, Series E, vol. 308, p. 309.
Devincre, B., Kubin, L.P., Lemarchand, C., Madec, R., 2001. Mesoscopic simulations of plastic deformation. Mater. Sci. Eng. A 309, 211–219.
Domain, C., Monnet, G., 2005. Simulation of screw dislocation motion in iron by molecular dynamics simulations. Phys. Rev. Lett. 95, 215506.
Dorn, J.E., Rajnak, S., 1964. Nucleation of kink pairs and the Peierls' mechanism of plastic deformation. Trans. Metall. Soc. AIME 230, 1052–1064.
Ghosh, G., Olson, G.B., 2002. The isotropic shear modulus of multicomponent Fe-base solid solutions. Acta Mater. 50, 2655–2675.
Hirth, J.P., Lothe, L., 1982. Theory of Dislocations, second ed. Wiley Inter-Science, New York.
Kocks, U.F., Argon, A.S., Ashby, M.F., 1975. Thermodynamics and kinetics of slip. Prog. Mater. Sci. 191–288.
Kossowsky, R., Brown, N., 1966. Microyielding in iron at low temperatures. Acta Metall. 14, 131–139.

Kubin, L.P., 1976. The low temperature plastic deformation of bcc metals. Rev. Deform. Behav. Mater. 1, 243–288.
Kuramoto, E., Aono, Y., Kitaj ima, K., 1979. Thermally activated slip deformation of high purity iron single crystals between 4.2 K and 300 K. Scr. Metall. 13, 1039–1041.
Louchet, F., Kubin, L.P., 1979. Dislocation processes in bcc metals. Phys. Stat. Sol. A 56, 169–176.
Mendelev, M.I., Han, S.W., Srolovitz, D.J., Ackland, G.J., Sun, D.Y., Asta, M., 2003. Development of new interatomic potentials appropriate for crystalline and liquid iron. Philos. Mag. 83, 3977–3994.
Monnet, G., Devincre, B., Kubin, L.P., 2004. Dislocation study of prismatic slip systems and their interactions in hexagonal close packed metals: application to zirconium. Acta Mater. 52, 4317–4328.
Nabarro, F.R.N., 2003. One-dimensional models of thermal activation under shear stress. Philos. Mag. 83, 3047–3054.
Queyreau, S., Monnet, G., Devincre, B., 2009. Slip systems interactions in a iron determined by dislocation dynamics simulations. Int. J. Plasticity 25, 361–377.
Quesnel, D.J., Sato, A., Meshii, M., 1975. Solution softening and hardening in the iron-carbon system. Mater. Sci. Eng. 18, 199–208.
Schoeck, G., 1965. The activation energy of dislocation movement. Phys. Stat. Sol. 8, 499–507.
Schoeck, G., Nabarro, F.R.N., 1980. Thermodynamics and Thermal Activation of Dislocations. Dislocations in Solids, vol. 2. Amsterdam, North Holland, p. 67.
Seeger, A., Schiller, P., 1962. The formation and diffusion of kinks as the fundamental process of dislocation movement in internal friction measurements. Acta Metall. 10, 348–357.
Solomon, H.D., McMahon, C.J., 1966. Exhaustion hardening of iron. In: Work hardening – Metallurgical Society Conference, vol. 46. Gordon & Beach, New York, pp. 311–332.
Smidt, F.A., 1969. An analysis of thermally activated flow in α iron based on T–τ^* considerations. Acta Metall. 17, 381–392.
Spitzig, W.A., Keh, A.S., 1970a. Orientation dependence of the train-rate sensitivity and thermally activated flow in iron single crystals. Acta Metall. 18, 1021–1033.
Spitzig, W.A., Keh, A.S., 1970b. The effect of orientation and temperature on the plastic flow properties of iron single crystals. Acta Metall. 18, 611–622.
Spitzig, W.A., 1973. The effects of orientation, temperature and strain rate on deformation of Fe–0.16 wt.%Ti single crystals. Mater. Sci. Eng. 12, 191–202.
Stein, D.F., Low, J.R., Seybolt, A.U., 1963. The mechanical properties of iron single crystals containing less than 5×10^{-3} ppm carbon. Acta Metall. 11, 1253–1262.
Tang, M., Kubin, L.P., Canova, G.R., 1998. Dislocation mobility and the mechanical response of bcc single crystals: a mesoscopic approach. Acta Mater. 46, 3221–3235.
Wen, M., Ngan, A.H.W., 2000. Atomistic simulation of kink-pairs of screw dislocations in body-centered cubic iron. Acta Mater. 48, 4255–4265.
Yang, L.H., Moriarty, J.A., 2001. Kink-pair mechanisms for a/2 $\langle 1\,1\,1 \rangle$ screw dislocation motion in bcc tantalum. Mater. Sci. Eng. A, 124–129.
Zbib, H.M., De la Rubia, T.D., Rhee, M., Hirth, J.P., 2000. 3D dislocation dynamics: stress–strain behavior and hardening mechanics in fcc and bcc metals. J. Nucl. Mater. 276, 154–165.